HHS Public Access

Author manuscript

Circulation. Author manuscript; available in PMC 2018 April 25.

Published in final edited form as:

Circulation. 2017 April 25; 135(17): 1632–1645. doi:10.1161/CIRCULATIONAHA.116.024470.

Sheet-Like Remodeling of the Transverse Tubular System in Human Heart Failure Impairs Excitation-Contraction Coupling and Functional Recovery by Mechanical Unloading

Thomas Seidel, MD, PhD[1], **Sutip Navankasattusas, PhD**[2], **Azmi Ahmad, BSc**[1,3], **Nikolaos A. Diakos, MD, PhD**[2], **Weining David Xu, MD**[4], **Martin Tristani-Firouzi, MD**[1], **Michael J. Bonios, MD, PhD**[4], **Iosif Taleb, MD**[4], **Dean Y. Li, MD, PhD**[2,4], **Craig H. Selzman, MD**[2,5], **Stavros G. Drakos, MD, PhD**[2,4,*], and **Frank B. Sachse, PhD**[1,3,*]

[1]Nora Eccles Harrison Cardiovascular Research and Training Institute, University of Utah, USA

[2]Molecular Medicine Program, University of Utah, USA

[3]Department of Bioengineering, University of Utah, USA

[4]Division of Cardiovascular Medicine, University of Utah, USA

[5]Division of Cardiothoracic Surgery, University of Utah, USA

Abstract

Background—Cardiac recovery in response to mechanical unloading by left ventricular assist devices (LVADs) has been demonstrated in subgroups of chronic heart failure (HF) patients. Hallmarks of HF are depletion and disorganization of the transverse tubular system (t-system) in cardiomyocytes. Here, we investigated remodeling of the t-system in human end-stage HF and its role in cardiac recovery.

Methods—Left ventricular biopsies were obtained from 5 donors (CTRL) and 26 chronic HF patients undergoing implantation of LVADs. Three-dimensional confocal microscopy and computational image analysis were applied to assess t-system structure, density, and distance of ryanodine receptor (RyR) clusters to the sarcolemma, including the t-system. Recovery of cardiac function in response to mechanical unloading was assessed by echocardiography during turn-down of the LVAD.

Results—The majority of HF myocytes showed remarkable t-system remodeling, particularly sheet-like invaginations of the sarcolemma. Circularity of t-system components was decreased in HF vs CTRL (0.37±0.01 vs 0.46±0.02, $p<0.01$), and the volume/length ratio was increased in HF

Corresponding Authors: Thomas Seidel, Nora Eccles Harrison Cardiovascular Research and Training Institute, University of Utah, 95 S 2000 E, Salt Lake City, UT 84112, Present address: Institute for Cellular and Molecular Physiology, Friedrich-Alexander-Universitaet Erlangen-Nuernberg, Waldstr. 6, 91054 Erlangen, Germany, thomas.seidel@fau.de, phone: +49-9131-8522303, fax: +49-9131-8522770. Stavros G. Drakos, University Hospital, Heart Failure Clinic, 50 N Medical Dr, Salt Lake City, UT 84132, stavros.drakos@hsc.utah.edu, twitter: @stavrosdrakos, phone: +1-801-585-5122. Frank B. Sachse, Nora Eccles Harrison Cardiovascular Research and Training Institute, University of Utah, 95 S 2000 E, Salt Lake City, UT 84112, frank.sachse@utah.edu, phone: +1-801-587-9514, fax: +1-801-581-3128.

*Shared senior authorship between S. G. Drakos and F. B. Sachse

Disclosures

None.

($0.36\pm0.01\mu m^2$ vs $0.25\pm0.02\mu m^2$, $p<0.0001$). T-system density was reduced in HF, leading to increased RyR-sarcolemma distances ($0.96\pm0.05\mu m$ vs $0.64\pm0.1\mu m$, $p<0.01$). Low RyR-sarcolemma distances at time of LVAD implantation predicted high post-LVAD left-ventricular ejection fractions (EF, $p<0.01$) and EF increase during unloading ($p<0.01$). EF in patients with pre-LVAD RyR-sarcolemma distances larger than 1μm did not improve following mechanical unloading. Additionally, calcium transients were recorded in field-stimulated isolated human cardiomyocytes and analyzed with respect to local t-system density. Calcium release in HF myocytes was restricted to regions proximal to the sarcolemma. Local calcium upstroke was delayed (23.9±4.9ms vs 10.3±1.7ms, $p<0.05$) and more asynchronous (18.1ms±1.5ms vs 8.9±2.2ms, $p<0.01$) in HF cells with low t-system density versus cells with high t-system density.

Conclusions—The t-system in end-stage human HF presents a characteristic novel phenotype consisting of sheet-like invaginations of the sarcolemma. Our results suggest that the remodeled t-system impairs excitation-contraction coupling and functional recovery during chronic LVAD unloading. An intact t-system at time of LVAD implantation may constitute a precondition and predictor for functional cardiac recovery following mechanical unloading.

Keywords

EC-coupling; T-tubules; ryanodine receptor; heart failure; recovery

Journal Subject Terms

Calcium Cycling/Excitation-Contraction Coupling; Cell Biology/Structural Biology; Contractile Function; Myocardial Regeneration; Prognosis; Heart Failure; Remodeling

Introduction

Chronic heart failure (HF) has a poor prognosis, despite advances in pharmacotherapy and mechanical circulatory support.[1] However, studies by us and others demonstrated that some HF patients are able to recover cardiac function after mechanical unloading with left ventricular (LV) assist devices (LVADs).[2–5] The feasibility of sustained recovery after LVAD removal has been demonstrated, with recovery rates ranging between 6% and 60%.[3, 6, 7] The large differences in recovery rates between studies are likely due to study design.[4] Yet, it remains unclear why some failing hearts show significant signs of functional recovery, while others do not. Mechanisms that allow or prevent functional cardiac recovery still need to be identified. Moreover, a biomarker or test for the potential of unloading-induced cardiac recovery would help clinicians to select the best candidates for LVAD implantation in hope of subsequent cardiac recovery. These patients might then follow a different clinical approach than patients with a low chance of recovery. The degrees of cardiac fibrosis and cell hypertrophy were suggested as possible predictors of cardiac recovery in studies with a limited number of samples,[8] but this has not been confirmed in other studies.[4] To date, no clinical or structural correlate can reliably identify patients who are likely to recover with LVAD therapy.

A microstructural feature of ventricular cardiomyocytes important for contractility is the transverse tubular system (t-system). The t-system consists of tubular invaginations of the

sarcolemma (t-tubules), predominantly located at the z-lines of sarcomeres. In human ventricular myocytes, t-tubules form a dense network of high spatial regularity. The t-system is crucial for efficient excitation-contraction coupling by bringing L-type calcium channels in the sarcolemma in proximity to clusters of ryanodine receptors (RyRs) in the sarcoplasmic reticulum. The spatial and functional grouping of L-type calcium channels with RyR clusters is referred to as a couplon. Couplons facilitate calcium-induced calcium release, a process during which calcium diffuses from the extracellular space to RyR channels, causing opening of RyR channels and subsequent calcium release from the sarcoplasmic reticulum. The resulting transient increase of cytosolic calcium subsequently triggers contraction.[9]

Several studies demonstrated that HF in humans and other mammals is associated with structural remodeling of the t-system.[10] Particularly, t-system depletion and changes in orientation have been described (see [11] for review). Reduced t-system density increases the number of RyR clusters which are not adjacent to sarcolemmal L-type calcium channels and thus not located within couplons. The distance between non-junctional RyR clusters and the closest sarcolemmal L-type calcium channels can be up to several micrometers. It is thought that this detachment causes inefficient excitation-contraction coupling in HF for mainly two reasons: [12–14] (1) RyR clusters detached from the sarcolemma, often labeled orphaned or non-junctional clusters, are exposed to a slower and smaller increase of calcium due to higher distance from L-type calcium channels. Thus, the open probability of non-junctional RyR clusters is reduced. This results in an overall decreased calcium release from the sarcoplasmic reticulum. (2) While junctional RyRs open quickly after opening of L-type calcium channels, non-junctional RyRs open after calcium has diffused over a much longer distance. This results in asynchronous calcium release.

Most of our knowledge about t-system remodeling in cardiac disease and its effects on excitation-contraction coupling is derived from animal studies. While three-dimensional microscopy and analyses of the t-system were applied in various animal models,[13, 15–19] most studies in humans relied on 2D images or did not investigate HF.[20] To date, major 3D features of t-system remodeling in human HF have not been investigated. Similarly, while many animal studies have demonstrated a relationship between remodeling of the t-system in failing hearts and alterations of excitation-contraction coupling,[21, 22] our insights into this relation in human HF are incomplete.

Animal models, however, do not fully reflect the complex long-term remodeling occurring in human HF. For example, a study on end-stage human HF suggested that decreased t-system density cannot be reversed by mechanical unloading,[23] which is in contrast to findings in a rodent model of mechanical unloading based on heterotopic abdominal heart transplantation.[21] Thus, it remains unclear whether the t-system is relevant for the response to clinical therapies.

Recent research established a correlation between t-system remodeling in ventricular cardiomyocytes and reduced contractility in failing human hearts.[24] Myocardial contraction was preserved in ventricular regions with intact t-system, but markedly reduced or absent in

regions with remodeled t-system. This leads to the question whether an intact t-system is required for functional recovery of failing human hearts.

To answer this question, we studied remodeling of the 3D t-system structure in patients with advanced HF and investigated effects of the remodeling on intracellular calcium release and cardiac recovery. In this paper we describe a novel type of t-system remodeling that is common in HF patients and associated with impaired excitation-contraction coupling. Further, we provide evidence that an intact t-system may be required for functional cardiac recovery following mechanical unloading.

Methods

Study Population and Tissue Acquisition

The study was approved by the institutional review boards of the University of Utah. Patient enrollment in this study has been described earlier.[23] Briefly, patients with advanced HF (NYHA classes III and IV) undergoing LVAD implantation were prospectively enrolled after giving written informed consent. Patients with infiltrative cardiomyopathy, hypertrophic cardiomyopathy or acute forms of HF, such as acute myocardial infarction, were prospectively excluded. Cardiac contractile function was assessed serially before and after unloading by measuring LV ejection fraction (EF) with standard echocardiography. Post-LVAD echoes were acquired during a 30-min turn-down of the revolutions per minute (rpm) of the assist device at 3 months after LVAD implantation.[25] This rpm turn-down echo is a standard procedure performed in order to evaluate the native heart function during regular loading conditions. Clinical investigators were blinded against results from histological analysis.

We collected tissue samples from the LV apical core at time of LVAD implantation from 26 patients with advanced HF. Based on published evidence by others and us, approximately 15–20% of patients respond to mechanical unloading with a considerable improvement in cardiac ejection fraction, resulting in post-LVAD EFs of 40% or more.[25] To cover this group of patients, we selected tissue samples from 10 consecutive patients with favorable myocardial response following LVAD unloading between 2012 and 2014 from the biorepository of the Utah Cardiac Recovery Program. The remaining 16 samples were selected from consecutive patients in the same time period without significant increase of LV EF. We also included tissue samples from matched regions of 5 donor hearts that were not allocated for transplantation due to non-cardiac reasons. For experiments in living isolated myocytes we obtained LV tissue samples from patients enrolled in the same clinical protocol at time of either LVAD implantation or heart transplantation, and from one donor heart.

Tissue Processing

Samples were snap-frozen in optimal cutting temperature (OCT) compound (Sakura Finetek Europe B.V., Alphen aan den Rijn, Netherlands) and stored at −80°C until usage. Tissue sections of 100μm thickness were acquired with a cryotome (CM 1950, Leica AG, Wetzlar, Germany), immediately immersed in 1% paraformaldehyde for 15min and subsequently washed in PBS. RyRs were immunolabeled (MA3-916 and A-21121, ThermoFisher

Scientific, Waltham, MA, USA), the sarcolemma and extracellular matrix stained with wheat germ agglutinin (WGA, ThermoFisher), and nuclei with DAPI as described previously.[15] To stain L-type Ca channels, we used the same protocol on non-fixed tissue slices and applied rabbit anti-CACNA1C (1:200, ab58552, abcam) as primary and goat anti-rabbit conjugated to AF488 (1:400, A27034, ThermoFisher) as secondary antibodies. Tissue slices were mounted on a glass slide, embedded in Fluoromount-G (#17984-25, Electron Microscopy Science, Hatfield, PA, USA) and then dried for at least 24h at room temperature and <40% relative humidity.

Three-dimensional Confocal Microscopy

A Leica SP8 TCS confocal microscope (Leica, Jena, Germany) was used to acquire 2–5 3D image stacks from each sample within 20μm from the cover slip in tissue regions containing myocytes. Investigators were not fully blinded against clinical data. See supplement for details of image acquisition and region selection.

Extracellular Dextran Perfusion

Isolated living myocytes from a failing heart were superfused with Tyrode's solution containing 5mg/ml of anionic dextran (10kDa) conjugated to fluorescein (FITC) as a volume marker of the extracellular space (Thermo Fisher, D1821). Three-dimensional images were acquired from these cells using channel 2 of the imaging protocol described above (488nm laser line).

Image Processing, Analysis and Visualization

Image stacks were filtered, deconvolved with measured point spread functions and corrected for depth-dependent attenuation.[26] The t-system and outer sarcolemma were extracted applying previously published methods for cell segmentation (Online Fig. 1).[27] We then determined eigenvectors and eigenvalues ($|\lambda_1| \geq |\lambda_2| \geq |\lambda_3|$)[28] and calculated cross-section circularity, defined as ratio of the two minor eigenvalues $|\lambda_3/\lambda_2|$, utilizing a published algorithm based on gradient vector flow.[29] All t-system and RyR measures were first averaged per image and subsequently per sample, resulting in one numerical value per measure and patient used for statistical analysis. Image analysis and processing steps were automated, using custom software scripts. Details are described in the supplement.

Cell Isolation, Imaging and Analysis of Calcium Transients

Methods for cell isolation, imaging and analyses of calcium transient are described in the supplemental methods. In short, we isolated cells from LV tissue samples obtained during LVAD implantation or heart transplantation. Cells were loaded with DI-8-ANEPPS and Fluo4, and subsequently imaged using 2D rapid scanning confocal microscopy. In the resulting image sequences, we measured the maximal upstroke velocity of cytosolic calcium and associated onset time in each pixel and related these measures to the distance from the nearest sarcolemma.

Statistical Analysis

If not indicated otherwise, statistical data are presented as mean±standard error. Statistical significance ($p<0.05$) was tested by two-sample unpaired t-test. Bonferroni-Holm correction for multiple comparisons was applied when testing for differences in RyR distribution. Paired t-test was used to compare pre-LVAD and post-LVAD clinical patient data. Linear regression models were created using the Matlab fitlm function with least-squares fitting. Linear models were considered significant versus respective constant models, if F-statistics yielded $p<0.05$.

Results

Study Population and Clinical Measurements

The study population comprised 26 chronic HF patients undergoing LVAD implantation. Pre-LVAD EF was 22±6%. Other clinical characteristics are summarized in Table 1. Two months after LVAD placement, hemodynamic measurements consistently showed decreases in right atrial pressure, pulmonary capillary wedge pressure, pulmonary artery pressure and pulmonary vascular resistance, which confirmed the effectiveness of mechanical unloading by the LVAD (Online Table 1).

Sheet-Like Remodeling of the T-System in HF Cardiomyocytes

We obtained LV biopsies for histological analysis by confocal microscopy from 26 patients at time of LVAD implantation and 5 normal donor hearts (control). Two-dimensional confocal scans covering up to $20mm^2$ consistently revealed a dense t-system in control samples, whereas many samples from failing hearts exhibited abundant remodeling of the t-system. In addition to local depletion, longitudinal components of t-system parallel to the cardiomyocyte's main axis were visible in 2D images (Fig. 1).

When examining and visualizing 3D images (Fig. 2), the t-system in control samples exhibited high density and nearly cylindrical membrane invaginations (Fig. 2A–D). In contrast, 3D visualization of HF samples revealed that the longitudinal structures seen in 2D images belonged to sparse and irregular sheet-like membrane invaginations (Fig. 2E–H). These transverse sheets (t-sheets) were easily identifiable in 3D reconstructions (Fig. 2G,H), but not in cross-sections (Fig. 2E,F). T-sheets presented as components of the t-system, which were widened mainly in parallel to the myocyte long axis. The major axis of t-sheets, however, was still oriented perpendicular to the outer sarcolemma and myocyte long axis. As a result, t-sheets appeared as longitudinal t-system components only in sections parallel to myocyte orientation, but were hardly distinguishable from normal t-tubules in sections perpendicular to myocyte orientation (Fig. 2F,G).

To quantify our visual observations, we applied 3D principal component analysis to individual connected components of the t-system extracted from a total of 102 image volumes (Fig. 3A,B). Circularity of t-tubule cross-sections (ratio of the two minor eigenvalues) was decreased (0.37±0.01 vs 0.46±0.02, $p<0.01$), while the volume/length ratio as a measure of t-tubule cross sectional area was increased in HF vs control ($0.36±0.01\mu m^2$ vs $0.25±0.02\mu m^2$, $p<0.0001$). These measures confirmed the typical shape of t-sheets in HF,

characterized by dilation of one cross-sectional dimension. In addition to this common feature, t-sheets presented with variations in size and curvature (Online Fig. 2). Moreover, the occurrence of t-sheets was associated with reduced t-system density, indicated by an increased mean intracellular distance to the sarcolemma in HF vs control (0.84±0.03μm vs 0.61±0.07μm, $p<0.01$, Fig. 3C) and a positive correlation of the volume/length ratio of t-system components with sarcolemma distance (Fig. 3D). Note that sarcolemma distance was calculated including the sarcolemma of the t-system.

To test whether t-sheets are connected to the extracellular space or might instead be an artifact of membrane staining with WGA, we carried out experiments with living cardiomyocytes isolated from failing hearts. Cardiomyocytes were placed into an extracellular bath containing a water-soluble, membrane-impermeable anionic dextran conjugated to fluorescein. The extracellular fluid immediately diffused into the t-system, but did not enter the cytosol. Three-dimensional images confirmed the presence of t-sheets in isolated myocytes and also their connection to the extracellular space (Fig. 3E). Immunostaining against L-type calcium channels in tissues from 3 controls and 3 failing hearts indicated the presence of clusters in t-sheets, similar to those seen in normal t-tubules (Online Fig. 3).

RyR-Sarcolemma Distance and Functional Myocardial Recovery

Next, we investigated the spatial relationship between RyR clusters and the t-system. While RyR clusters in control were predominantly located proximal to the sarcolemma (Fig. 4A,B), most HF samples exhibited a large number of RyR clusters distant from the sarcolemma (Fig. 4C–D). Quantitative image analysis showed an altered RyR distribution in HF, with a marked shift towards larger distances (Fig. 4E). In control cells 23% of RyRs were found >1μm from the sarcolemma, whereas this number increased to 44% in HF. Consequently, mean RyR-sarcolemma distance was significantly higher in HF than control (0.96±0.05μm vs 0.64±0.1μm, Fig. 4F).

To investigate the importance of t-system remodeling in cardiac recovery, we correlated the pre-LVAD RyR-sarcolemma distance from each patient with LV EF before and after mechanical unloading using linear regression models (Fig. 5A–C). No correlation was found with pre-LVAD EF ($p=0.8$ vs constant model), which means that cardiac contractile function at time of LVAD implantation was not directly associated with changes of the t-system. However, pre-LVAD t-system remodeling showed significant correlations with post-LVAD EF ($p<0.01$) and EF change during unloading by LVAD ($p<0.01$). The more pronounced the t-system remodeling was before mechanical unloading, the more unlikely was an increase in ejection fraction in response to unloading. Or, put differently, recovery of EF was more likely when the t-system was intact at time of LVAD implantation.

We found that patients with RyR-sarcolemma distances higher than 1μm hardly responded with increases in EF (Fig. 5C). Therefore, we grouped patients by low and high RyR-sarcolemma distance (<1μm, n=16 vs >1μm, n=10, Fig. 5D–H). Again, we did not find differences in pre-LVAD EF (20.7±1.8% vs 23.4±2%, $p=0.3$), but in post-LVAD EF (37.8±3% vs 24.9±2.4%, $p<0.01$) and a striking difference in EF change, with almost no recovery of EF when RyR-sarcolemma was >1μm (17.1±3.6% vs 1.4±1.6%, $p<0.01$). The

recovery of EF ranged from 0% to 38% in patients with RyR-sarcolemma distance <1μm, but only from −5% to 5% in patients with RyR-sarcolemma distance >1μm. A paired t-test between post- and pre-LVAD EF indicated recovery if RyR-sarcolemma distance was low ($p<0.001$), but no recovery if high ($p=0.36$). Thus, recovery of EF occurred only in patients with low degrees of t-system remodeling.

Additionally, we found that patients with high RyR-sarcolemma distances had a longer history of HF symptoms than patients with low distances (6.5±1.9 vs 1.8±0.5 years, $p<0.01$). To evaluate whether increased RyR-sarcolemma distances resulted from reduced t-system density we compared mean intracellular sarcolemma distances. We found high (0.9±0.05μm, $p<0.01$) and low (0.75±0.03μm) intracellular sarcolemma distances in groups with high and low RyR-sarcolemma distances, respectively. This indicates that increased distances between RyR clusters and the sarcolemma were primarily due to a loss of t-tubules rather than a redistribution of RyRs. Moreover, the occurrence of t-sheets was accompanied by increased RyR-sarcolemma distances (Online Fig. 4).

We explored the relationship of RyR-sarcolemma distance with clinical measures which have been related to cardiac recovery in previous work, [25, 30] (Online Table 2). These measures included LV mass and volume as well as measures of diastolic function. Our analyses suggest that low pre-unloading RyR-sarcolemma distance, i.e. an intact t-system, correlates with recovery of LV dimensions and diastolic function.

Asynchronous Calcium Transients in Remodeled Myocytes

To study effects of t-system remodeling on excitation-contraction coupling, we analyzed intracellular sarcolemma distances and the initial phase of calcium transients in 15 isolated LV cardiomyocytes from 6 HF patients. An example cell labeled with di-8-ANEPPS for the sarcolemma, including the t-system (Fig. 6A), revealed t-sheets as observed in fixed tissue samples (Figs. 2F and 4D). When myocytes were field-stimulated at 37°C, we found that calcium transients were restricted to regions proximal to t-sheets (Fig. 6B). Due to the low t-system density, this resulted in inhomogeneous local onset times of calcium increase (Fig. 6C) and inhomogeneous calcium upstroke velocities (Fig. 6D). In the presented example cell, local onset time determined for each intracellular pixel increased monotonically with sarcolemma distance (Fig. 6E), while upstroke velocity decreased with distance (Fig. 6F). The increase of onset time and decrease of upstroke velocity with distance was present in all analyzed cells (Fig. 6G,H).

Next, similar to the analysis of tissue samples, we grouped cells by low (<1μm, n=8) and high (>1μm, n=7) intracellular sarcolemma distance as a measure of high and low t-system density, respectively. The two groups revealed significant differences in means and standard deviations of onset time. Onset time was increased for low t-system density (23.9±4.9ms vs 10.3±1.7ms, $p<0.05$), which indicates delayed or absent calcium release (Fig. 6I). Standard deviation of onset time (Fig. 6J), a measure of asynchrony of calcium release, was also increased in cells with low t-system density (18.1±1.5ms vs 8.9±2.2ms, $p<0.01$). Thus, t-system loss was associated with inhomogeneous and delayed calcium release. A homogeneous calcium transient from a control cell is presented in Online Fig. 5.

Discussion

Three-dimensional imaging of ventricular cardiomyocytes obtained from HF patients undergoing LVAD implantation revealed a previously unknown phenotype of the t-system. This phenotype consists of sheet-like rather than tubular membrane invaginations. We named these t-system components t-sheets to distinguish them from transverse and less common axial components with a tubular shape. In most cases the major axis of t-sheets runs transverse to the myocyte long axis (Fig. 2G), similar to a normal t-tubule. The longitudinal appearance in cross-sections parallel to the myocyte long axis (Figs. 1D,E and 2F) results from dilation of t-sheets along this axis leading to a non-tubular, sheet-like shape (Fig. 2H). T-sheets were arranged less regularly than normal t-tubules, and were commonly sparsely distributed. Myocytes with t-sheets were frequently present in the HF tissues analyzed in this study, but not in control. They were associated with reduced t-system density, increased RyR-sarcolemma distances and spatiotemporal heterogeneity of intracellular calcium release. Importantly, large RyR-sarcolemma distances at time of LVAD implantation indicated only marginal or absent functional cardiac recovery during the following mechanical unloading. Conversely, an intact t-system structure was a predictor of cardiac recovery in response to mechanical unloading by LVAD.

T-Sheets as a Novel Type of T-System Remodeling

Remodeling of the t-system in cardiac disease has been reported for various species and etiologies. Previous studies on human heart disease suggested that remodeling comprises enlarged axial t-tubules,[31] loss of t-system,[32] and dilation of peripheral t-tubules.[33] Commonly, these studies relied on 2D images acquired with confocal or electron microscopy. The resulting images represent cross-sections through the t-system, which impedes identification of sheet-like structures. For instance, the cross-sections through t-sheets could be interpreted as axial t-tubules, i.e. running parallel to the longitudinal cell axis.[31] Here, we applied 3D confocal microscopy, computational analysis and image reconstructions, which revealed remodeling of t-tubules to sheet-like t-system components in advanced human HF. Our visual findings were confirmed by 3D geometrical measures applied to the t-system. Similar to 2D analysis of the area/skeleton ratio in a recent study on t-system structure in human dilated cardiomyopathy,[24] we applied the volume-to-length ratio of t-tubules as a 3D measure, which indicated widening of t-tubules in HF. As a second measure, which is more specific for the shape, we used the cross-section circularity of t-tubules. While the circularity of a perfectly circular cross-section is 1, the mean circularity of t-tubules in human donor hearts was near 0.5. This is in agreement with previous work on t-tubules in healthy rabbit ventricular myocytes.[34] Here, we found that cross-section circularity was significantly decreased in HF, indicating that t-tubules were remodeled to more elliptic or sheet-like components.

We excluded the possibilities that t-sheets are intracellular vesicles or a processing artifact by confirming them in living isolated myocytes with two different labeling strategies (Figs. 3E and 6A). We ruled out that the observed sheets are separated from the extracellular space and represent vesicles, by demonstrating that the cavities of sheets are accessible to extracellular fluids using a membrane-impermeable extracellular marker (Fig. 3E).[17]

Additionally, the lipophilic dye Di-8-ANEPPS effectively stained t-tubules and t-sheets. Other indicators of t-sheets as functional t-system components were the initiation of calcium transients proximal to t-sheets (Fig. 6) and the presence of L-type calcium channel clusters in the t-sheet membrane (Online Fig. 3). Therefore, our studies strongly suggest that t-sheets belong to the sarcolemma, signal electrical activation into the interior of the cell and contribute to excitation-contraction coupling, similar to normal t-tubules. Also, our images and analyses (Fig. 4) suggest that a fraction of RyRs is located proximal to t-sheets, which is a fundamental requirement for the formation of couplons.

A limitation of our approaches is that confocal microscopy does not resolve the nano-structure of t-sheets. T-sheets might therefore represent t-tubules spaced tightly below the resolution limit of confocal microscopy. However, such tight spacing seems unlikely because studies in human HF with 2D electron microscopy described longitudinal t-system components, but never tightly spaced t-tubules.[31]

Potential Mechanisms Underlying T-System Remodeling

Our studies are preparatory for investigations on mechanisms underlying sheet-like remodeling of the t-system. In previous work on canine models of dyssynchronous HF, we proposed that changes in regional strain profiles affect t-system structure and maintenance.[15] In dyssynchronous HF, changes in regional strain profiles are caused by interventricular dyssynchrony due to left bundle branch block, which is common in HF patients. Furthermore, many types of HF are associated with fibrosis, which is a frequent finding also in our patient population (e.g. Figs. 1C and 2E). Fibrosis is known to stiffen the myocardium[35] and, thus, will alter local strain profiles, possibly triggering sheet-like remodeling. An alternative potential mechanism is related to the increase in wall stress resulting from elevated LV diastolic pressure and increased LV diameters in LVAD patients (Online Table 1). Increased wall stress has recently been suggested to underlie t-system remodeling in rats.[36] However, while an association of changes in t-system with myocardial wall stress in-vivo and in-vitro was demonstrated in this study, the type of remodeling, i.e. de-tubulation, was different from the findings in our study.

Several proteins have been related to t-system assembly, maintenance and remodeling in cardiac diseases, for example junctophilin-2, caveolin-3, amphiphysin-2, and telethonin.[11, 37–40] Involvement of the cytoskeleton has been suggested as well. For example, it was reported recently that microtubule densification in cardiomyocytes, which is commonly observed in heart failure, causes t-system remodeling in mice by impacting junctophilin-2 traffic.[41] Another study related t-system remodeling to p21-activated kinase (PAK1), a serine-threonine kinase involved in cytoskeletal organization.[42] Future studies should focus on these mechanisms in human heart failure.

Nevertheless, it is generally difficult to determine if changes in t-system-related proteins are the primary cause of t-system remodeling or rather a result of t-tubule loss in HF. This is particularly challenging because t-system remodeling and HF appear strongly intertwined and can hardly be investigated independently in patients. One way to overcome these challenges is the development of in-vitro and in-vivo models with more control over tissue remodeling and environmental conditions. However, results from these models can be

applied only with caution to human HF and thus need to be confirmed in HF patients for the following reasons: (1) HF in humans usually develops over a much longer time than in animal models, leading to long-term remodeling and associated functional changes. (2) The t-system in humans and certain animals, especially rodents, differs significantly.[43] (3) The t-system is commonly not well preserved in in-vitro models.[44]

T-System Remodeling and Excitation-Contraction Coupling

T-System remodeling in our studies of human HF led to increased RyR-sarcolemma distances reflecting a decreased number of junctional RyR clusters and increased number of non-junctional RyR clusters. This is obvious in Fig. 4D, which shows a high percentage of non-junctional RyR clusters, i.e. distal from the sarcolemma. Non-junctional RyR clusters are not located in a junctional space and not associated with L-type calcium channels. Therefore, non-junctional RyR clusters need to be activated by calcium diffusing into the vicinity of these clusters. In all likelihood, the rise will be delayed and much smaller than in couplons. Thus, activation of non-junctional RyR clusters will be delayed and the probability of activation will be reduced. The resulting calcium transients within cells will be inhomogeneous and attenuated.

In agreement with this line of thought, we found an increased local onset time of calcium transients and decreased maximal upstroke velocities with distance to the sarcolemma in human HF cells. Accordingly, decreased t-system density was associated with increased mean and standard deviation of onset time, which describes that calcium release was delayed and inhomogeneous. This would be expected from a higher fraction of non-junctional RyRs. These findings are in agreement with our previous studies on partially de-tubulated rabbit ventricular myocytes.[14] The consequence of the observed inhomogeneous calcium release would be reduced efficiency of cellular contraction, translating into reduced cardiac contractility. This fits well to our observation that only patients with an intact t-system structure can achieve high ejection fractions after unloading.

We note that attenuation of calcium transients in HF is commonly explained by reduced content and release of calcium from the sarcoplasmic reticulum. Reduced sarcoplasmic calcium content in HF is thought to be the result of down-regulation of the sarcoplasmic/endoplasmic reticulum calcium ATPase (SERCA) and up-regulation the sodium-calcium exchanger (NCX).[45] In agreement, calcium transients in our HF cells were uniformly attenuated. However, by comparing HF cells with relatively high t-system density to HF cells with low t-system density (Fig. 6), we were able to provide new insight into causes underlying the heterogeneity of calcium transients in human HF. We propose that t-system remodeling affects calcium transients in addition to changes in cellular SERCA, NCX or L-type calcium levels by reducing their efficiency. This hypothesis could be tested by directly relating t-system density to cellular calcium fluxes.

T-System Remodeling and Recovery

Restoration of t-system structure was demonstrated, for example, in canine models of cardiac resynchronization therapy.[13] Studies on a rodent model of HF suggested that mechanical unloading restores t-system structure and calcium-induced calcium release.[21] In

contrast, our previous study on a similar patient cohort as presented here suggested that RyR-sarcolemma distances do not change during mechanical unloading.[23] This implies that mechanical unloading in advanced human HF does not lead to restoration of normal t-system structure.

Persistent t-system remodeling may therefore explain why patients with high RyR-sarcolemma distances are not able to improve EF in response to LVAD unloading (Fig. 7). At time of LVAD implantation t-system remodeling did not correlate with EF, suggesting that reversible mechanisms contributed to the poor contractility found in these patients. For example cardiac metabolism[46], the response to β-adrenergic stimulation[47, 48] or NCX expression[45] have been reported to improve in response to mechanical unloading in HF patients.

Our finding that patients with high RyR-sarcolemma distances had longer histories of HF symptoms (Fig. 5G) suggests that t-system remodeling progresses over time. This is also in agreement with and may explain findings from other studies reporting that cardiac recovery is more likely in patients with shorter histories of chronic HF.[3, 4, 7]

A limitation of our study is that investigators acquiring images were not always blinded against clinical data. In some cases, it was known whether a patient had responded with signs of cardiac recovery and thus investigators might be subconsciously biased in their selection of image regions. However, image regions were preselected by bright-field microscopy, by which the t-system and RyRs cannot be identified. We therefore believe that investigator bias was negligible.

Clinical Perspective

The correlation between the degree of t-system remodeling before LVAD implantation and subsequent recovery of contractile function found in this study may render the t-system a useful histological parameter to characterize HF and predict recovery. The series of protocols required to facilitate cardiac recovery include: (1) serially monitoring function of the unloaded heart; (2) continuously adjusting adjuvant anti-remodeling drugs to maximize their doses and efficacy; and (3) standardizing criteria for LVAD explantation and cardiac recovery. Establishing criteria for LVAD explantation remains challenging because standard clinical data, e.g. echocardiographic parameters, age, comorbidities, etiology and duration of HF, are weak predictors of recovery.[4, 49] Thus, there is an urgent need for additional predictors to improve patient selection for LVAD explantation. Using both established clinical data and novel biomarkers, for example the degree of t-system remodeling, may therefore help to acquire relevant information for patient selection.

Conclusion

We conclude that an intact t-system is required, but not sufficient for significant functional improvement following mechanical unloading. Assessing t-system structure at time of LVAD implantation, together with clinical data, may help to identify patients who will recover cardiac function.

Supplementary Material

Refer to Web version on PubMed Central for supplementary material.

Acknowledgments

We thank Dr. Kenneth Spitzer for help with myocyte isolation, Dr. John Bridge for insightful discussions as well as Mrs. Nancy Allen and Mr. Bruce Steadman for technical support. We are in debt to the Intermountain Donor Services for help in acquiring myocardial tissue from donor hearts.

Sources of Funding

This work was supported by NIH R01HL132067 (SDG, FBS), AHA fellowship 14POST19820010 (TS), NIH R01HL094464 (FBS), the Nora Eccles Treadwell Foundation (FBS), Doris Duke Foundation Clinical Scientist Grant 2013108 (SGD), AHA CV Genome Phenome Discovery Grant (SGD) and the NIH NCRR/CCTS-UL1-RR025764 and C06-RR11234 (SGD).

References

1. Mozaffarian D, Benjamin EJ, Go AS, Arnett DK, Blaha MJ, Cushman M, Das SR, de Ferranti S, Despres JP, Fullerton HJ, Howard VJ, Huffman MD, Isasi CR, Jimenez MC, Judd SE, Kissela BM, Lichtman JH, Lisabeth LD, Liu S, Mackey RH, Magid DJ, McGuire DK, Mohler ER 3rd, Moy CS, Muntner P, Mussolino ME, Nasir K, Neumar RW, Nichol G, Palaniappan L, Pandey DK, Reeves MJ, Rodriguez CJ, Rosamond W, Sorlie PD, Stein J, Towfighi A, Turan TN, Virani SS, Woo D, Yeh RW, Turner MB. American Heart Association Statistics C, Stroke Statistics S. Executive Summary: Heart Disease and Stroke Statistics-2016 Update: A Report From the American Heart Association. Circulation. 2016; 133:447–454. [PubMed: 26811276]
2. Drakos SG, Terrovitis JV, Anastasiou-Nana MI, Nanas JN. Reverse remodeling during long-term mechanical unloading of the left ventricle. J Mol Cell Cardiol. 2007; 43:231–42. [PubMed: 17651751]
3. Birks EJ, George RS, Hedger M, Bahrami T, Wilton P, Bowles CT, Webb C, Bougard R, Amrani M, Yacoub MH, Dreyfus G, Khaghani A. Reversal of severe heart failure with a continuous-flow left ventricular assist device and pharmacological therapy: a prospective study. Circulation. 2011; 123:381–390. [PubMed: 21242487]
4. Drakos SG, Kfoury AG, Stehlik J, Selzman CH, Reid BB, Terrovitis JV, Nanas JN, Li DY. Bridge to recovery: understanding the disconnect between clinical and biological outcomes. Circulation. 2012; 126:230–241. [PubMed: 22777666]
5. Birks EJ, Tansley PD, Hardy J, George RS, Bowles CT, Burke M, Banner NR, Khaghani A, Yacoub MH. Left ventricular assist device and drug therapy for the reversal of heart failure. N Engl J Med. 2006; 355:1873–1884. [PubMed: 17079761]
6. Maybaum S, Mancini D, Xydas S, Starling RC, Aaronson K, Pagani FD, Miller LW, Margulies K, McRee S, Frazier OH, Torre-Amione G, Group LW. Cardiac improvement during mechanical circulatory support: a prospective multicenter study of the LVAD Working Group. Circulation. 2007; 115:2497–2505. [PubMed: 17485581]
7. Dandel M, Weng Y, Siniawski H, Stepanenko A, Krabatsch T, Potapov E, Lehmkuhl HB, Knosalla C, Hetzer R. Heart failure reversal by ventricular unloading in patients with chronic cardiomyopathy: criteria for weaning from ventricular assist devices. European heart journal. 2011; 32:1148–1160. [PubMed: 20929978]
8. Bruckner BA, Razeghi P, Stetson S, Thompson L, Lafuente J, Entman M, Loebe M, Noon G, Taegtmeyer H, Frazier OH, Youker K. Degree of cardiac fibrosis and hypertrophy at time of implantation predicts myocardial improvement during left ventricular assist device support. J Heart Lung Transplant. 2004; 23:36–42. [PubMed: 14734125]
9. Fabiato A. Mechanism of Ca2+-induced release of Ca2+ from the sarcoplasmic reticulum of a skinned cardiac cell from the rat ventricle. J Physiol. 1985; 358:58P.
10. Brette F, Orchard C. T-tubule function in mammalian cardiac myocytes. Circ Res. 2003; 92:1182–1192. [PubMed: 12805236]

11. Guo A, Zhang C, Wei S, Chen B, Song LS. Emerging mechanisms of T-tubule remodelling in heart failure. Cardiovasc Res. 2013; 98:204–215. [PubMed: 23393229]
12. Heinzel FR, Bito V, Biesmans L, Wu M, Detre E, von Wegner F, Claus P, Dymarkowski S, Maes F, Bogaert J. Remodeling of T-Tubules and Reduced Synchrony of Ca2+ Release in Myocytes From Chronically Ischemic Myocardium. Circ Res. 2008; 102:338. [PubMed: 18079411]
13. Sachse FB, Torres NS, Savio-Galimberti E, Aiba T, Kass DA, Tomaselli GF, Bridge JH. Subcellular Structures and Function of Myocytes Impaired During Heart Failure Are Restored by Cardiac Resynchronization Therapy. Circ Res. 2012; 110:588–597. [PubMed: 22253411]
14. Torres NS, Sachse FB, Izu LT, Goldhaber JI, Spitzer KW, Bridge JH. A modified local control model for Ca2+ transients in cardiomyocytes: junctional flux is accompanied by release from adjacent non-junctional RyRs. J Mol Cell Cardiol. 2014; 68:1–11. [PubMed: 24389341]
15. Li H, Lichter JG, Seidel T, Tomaselli GF, Bridge JH, Sachse FB. Cardiac Resynchronization Therapy Reduces Subcellular Heterogeneity of Ryanodine Receptors, T-Tubules, and Ca2+ Sparks Produced by Dyssynchronous Heart Failure. Circ Heart Fail. 2015; 8:1105–1114. [PubMed: 26294422]
16. Soeller C, Cannell MB. Examination of the transverse tubular system in living cardiac rat myocytes by 2-photon microscopy and digital image-processing techniques. Circ Res. 1999; 84:266–275. [PubMed: 10024300]
17. Savio-Galimberti E, Frank J, Inoue M, Goldhaber JI, Cannell MB, Bridge JH, Sachse FB. Novel features of the rabbit transverse tubular system revealed by quantitative analysis of three-dimensional reconstructions from confocal images. Biophys J. 2008; 95:2053–2062. [PubMed: 18487298]
18. Wong J, Baddeley D, Bushong EA, Yu Z, Ellisman MH, Hoshijima M, Soeller C. Nanoscale distribution of ryanodine receptors and caveolin-3 in mouse ventricular myocytes: dilation of t-tubules near junctions. Biophys J. 2013; 104:L22–L24. [PubMed: 23746531]
19. Rog-Zielinska EA, Johnston CM, O'Toole ET, Morphew M, Hoenger A, Kohl P. Electron tomography of rabbit cardiomyocyte three-dimensional ultrastructure. Prog Biophys Mol Biol. 2016; 121:77–84. [PubMed: 27210305]
20. Sulkin MS, Yang F, Holzem KM, Van Leer B, Bugge C, Laughner JI, Green K, Efimov IR. Nanoscale three-dimensional imaging of the human myocyte. J Struct Biol. 2014; 188:55–60. [PubMed: 25160725]
21. Ibrahim M, Navaratnarajah M, Siedlecka U, Rao C, Dias P, Moshkov AV, Gorelik J, Yacoub MH, Terracciano CM. Mechanical unloading reverses transverse tubule remodelling and normalizes local Ca(2+)-induced Ca(2+)release in a rodent model of heart failure. Eur J Heart Fail. 2012; 14:571–580. [PubMed: 22467752]
22. Shah SJ, Aistrup GL, Gupta DK, O'Toole MJ, Nahhas AF, Schuster D, Chirayil N, Bassi N, Ramakrishna S, Beussink L, Misener S, Kane B, Wang D, Randolph B, Ito A, Wu M, Akintilo L, Mongkolrattanothai T, Reddy M, Kumar M, Arora R, Ng J, Wasserstrom JA. Ultrastructural and cellular basis for the development of abnormal myocardial mechanics during the transition from hypertension to heart failure. Am J Physiol Heart Circ Physiol. 2014; 306:H88–H100. [PubMed: 24186100]
23. Diakos NA, Selzman CH, Sachse FB, Stehlik J, Kfoury AG, Wever-Pinzon O, Catino A, Alharethi R, Reid BB, Miller DV, Salama M, Zaitsev AV, Shibayama J, Li H, Fang JC, Li DY, Drakos SG. Myocardial atrophy and chronic mechanical unloading of the failing human heart: implications for cardiac assist device-induced myocardial recovery. Journal of the American College of Cardiology. 2014; 64:1602–1612. [PubMed: 25301465]
24. Crossman DJ, Young AA, Ruygrok PN, Nason GP, Baddelely D, Soeller C, Cannell MB. T-tubule disease: Relationship between t-tubule organization and regional contractile performance in human dilated cardiomyopathy. J Mol Cell Cardiol. 2015; 84:170–178. [PubMed: 25953258]
25. Drakos SG, Wever-Pinzon O, Selzman CH, Gilbert EM, Alharethi R, Reid BB, Saidi A, Diakos NA, Stoker S, Davis ES, Movsesian M, Li DY, Stehlik J, Kfoury AG. Investigators U. Magnitude and time course of changes induced by continuous-flow left ventricular assist device unloading in chronic heart failure: insights into cardiac recovery. Journal of the American College of Cardiology. 2013; 61:1985–1994. [PubMed: 23500219]

26. Seidel T, Edelmann JC, Sachse FB. Analyzing Remodeling of Cardiac Tissue: A Comprehensive Approach Based on Confocal Microscopy and 3D Reconstructions. Ann Biomed Eng. 2016; 44:1436–1448. [PubMed: 26399990]
27. Seidel T, Dräbing T, Seemann G, Sachse FB. A semi-automatic approach for segmentation of three-dimensional microscopic image stacks of cardiac tissue. Lecture Notes in Computer Science. 2013; 7945:300–307.
28. McNary TG, Bridge JH, Sachse FB. Strain transfer in ventricular cardiomyocytes to their transverse tubular system revealed by scanning confocal microscopy. Biophys J. 2011; 100:L53–L55. [PubMed: 21575564]
29. Bauer C, Bischof H. A novel approach for detection of tubular objects and its application to medical image analysis. Joint Pattern Recognition Symposium. 2008:163–172.
30. Wever-Pinzon O, Drakos SG, McKellar SH, Horne BD, Caine WT, Kfoury AG, Li DY, Fang JC, Stehlik J, Selzman CH. Cardiac Recovery During Long-Term Left Ventricular Assist Device Support. Journal of the American College of Cardiology. 2016; 68:1540–1553. [PubMed: 27687196]
31. Kaprielian RR, Stevenson S, Rothery SM, Cullen MJ, Severs NJ. Distinct patterns of dystrophin organization in myocyte sarcolemma and transverse tubules of normal and diseased human myocardium. Circulation. 2000; 101:2586–2594. [PubMed: 10840009]
32. Lyon AR, MacLeod KT, Zhang Y, Garcia E, Kanda GK, Lab MJ, Korchev YE, Harding SE, Gorelik J. Loss of T-tubules and other changes to surface topography in ventricular myocytes from failing human and rat heart. Proc Natl Acad Sci U S A. 2009; 106:6854–6859. [PubMed: 19342485]
33. Crossman DJ, Ruygrok PR, Soeller C, Cannell MB. Changes in the organization of excitation-contraction coupling structures in failing human heart. PLoS One. 2011; 6:e17901. [PubMed: 21408028]
34. McNary TG, Spitzer KW, Holloway H, Bridge JH, Kohl P, Sachse FB. Mechanical modulation of the transverse tubular system of ventricular cardiomyocytes. Prog Biophys Mol Biol. 2012; 110:218–225. [PubMed: 22884710]
35. Doering CW, Jalil JE, Janicki JS, Pick R, Aghili S, Abrahams C, Weber KT. Collagen network remodelling and diastolic stiffness of the rat left ventricle with pressure overload hypertrophy. Cardiovasc Res. 1988; 22:686–695. [PubMed: 2978464]
36. Frisk M, Ruud M, Espe EK, Aronsen JM, Roe AT, Zhang L, Norseng PA, Sejersted OM, Christensen GA, Sjaastad I, Louch WE. Elevated ventricular wall stress disrupts cardiomyocyte t-tubule structure and calcium homeostasis. Cardiovasc Res. 2016; 112:443–451. [PubMed: 27226008]
37. Ibrahim M, Siedlecka U, Buyandelger B, Harada M, Rao C, Moshkov A, Bhargava A, Schneider M, Yacoub MH, Gorelik J, Knoll R, Terracciano CM. A critical role for Telethonin in regulating t-tubule structure and function in the mammalian heart. Hum Mol Genet. 2013; 22:372–383. [PubMed: 23100327]
38. Landstrom AP, Kellen CA, Dixit SS, van Oort RJ, Garbino A, Weisleder N, Ma J, Wehrens XH, Ackerman MJ. Junctophilin-2 expression silencing causes cardiocyte hypertrophy and abnormal intracellular calcium-handling. Circ Heart Fail. 2011; 4:214–223. [PubMed: 21216834]
39. Laury-Kleintop LD, Mulgrew JR, Heletz I, Nedelcoviciu RA, Chang MY, Harris DM, Koch WJ, Schneider MD, Muller AJ, Prendergast GC. Cardiac-specific disruption of Bin1 in mice enables a model of stress- and age-associated dilated cardiomyopathy. J Cell Biochem. 2015; 116:2541–2551. [PubMed: 25939245]
40. Caldwell JL, Smith CE, Taylor RF, Kitmitto A, Eisner DA, Dibb KM, Trafford AW. Dependence of cardiac transverse tubules on the BAR domain protein amphiphysin II (BIN-1). Circ Res. 2014; 115:986–996. [PubMed: 25332206]
41. Zhang C, Chen B, Guo A, Zhu Y, Miller JD, Gao S, Yuan C, Kutschke W, Zimmerman K, Weiss RM, Wehrens XH, Hong J, Johnson FL, Santana LF, Anderson ME, Song LS. Microtubule-mediated defects in junctophilin-2 trafficking contribute to myocyte transverse-tubule remodeling and Ca2+ handling dysfunction in heart failure. Circulation. 2014; 129:1742–1750. [PubMed: 24519927]

42. DeSantiago J, Bare DJ, Ke Y, Sheehan KA, Solaro RJ, Banach K. Functional integrity of the T-tubular system in cardiomyocytes depends on p21-activated kinase 1. J Mol Cell Cardiol. 2013; 60:121–128. [PubMed: 23612118]

43. Jayasinghe I, Crossman D, Soeller C, Cannell M. Comparison of the organization of T-tubules, sarcoplasmic reticulum and ryanodine receptors in rat and human ventricular myocardium. Clin Exp Pharmacol Physiol. 2012; 39:469–476. [PubMed: 21790719]

44. Banyasz T, Lozinskiy I, Payne CE, Edelmann S, Norton B, Chen B, Chen-Izu Y, Izu LT, Balke CW. Transformation of adult rat cardiac myocytes in primary culture. Exp Physiol. 2008; 93:370–382. [PubMed: 18156167]

45. Chaudhary KW, Rossman EI, Piacentino V 3rd, Kenessey A, Weber C, Gaughan JP, Ojamaa K, Klein I, Bers DM, Houser SR, Margulies KB. Altered myocardial Ca2+ cycling after left ventricular assist device support in the failing human heart. Journal of the American College of Cardiology. 2004; 44:837–845. [PubMed: 15312868]

46. Chokshi A, Drosatos K, Cheema FH, Ji R, Khawaja T, Yu S, Kato T, Khan R, Takayama H, Knoll R, Milting H, Chung CS, Jorde U, Naka Y, Mancini DM, Goldberg IJ, Schulze PC. Ventricular assist device implantation corrects myocardial lipotoxicity, reverses insulin resistance, and normalizes cardiac metabolism in patients with advanced heart failure. Circulation. 2012; 125:2844–2853. [PubMed: 22586279]

47. Klotz S, Barbone A, Reiken S, Holmes JW, Naka Y, Oz MC, Marks AR, Burkhoff D. Left ventricular assist device support normalizes left and right ventricular beta-adrenergic pathway properties. Journal of the American College of Cardiology. 2005; 45:668–676. [PubMed: 15734609]

48. Dipla K, Mattiello JA, Jeevanandam V, Houser SR, Margulies KB. Myocyte recovery after mechanical circulatory support in humans with end-stage heart failure. Circulation. 1998; 97:2316–2322. [PubMed: 9639375]

49. Drakos SG, Mehra MR. Clinical myocardial recovery during long-term mechanical support in advanced heart failure: Insights into moving the field forward. J Heart Lung Transplant. 2016; 35:413–420. [PubMed: 26922277]

Clinical Perspective

What is new?

- With sheet-like rather than tubular membrane invaginations, the transverse tubular system (t-system) of ventricular myocytes of human end-stage failing hearts exhibits a previously unknown remodeled phenotype.
- Sheet-like t-system remodeling leads to increased distances of ryanodine receptors to the sarcolemma, which causes heterogeneous intracellular calcium release and, consequently, inefficient excitation-contraction coupling.
- High degrees of t-system remodeling at time of left-ventricular assist device (LVAD) implantation are associated with absence of functional cardiac recovery during mechanical unloading, whereas preserved t-system structure is associated with recovery.

What are the clinical implications?

- T-system remodeling and impaired excitation-contraction coupling may prevent functional cardiac recovery in response to mechanical unloading by LVADs.
- Therefore, cardiac recovery during unloading may require an intact t-system at time of LVAD implantation.
- Characterizing the t-system may help to identify patients with high probability of functional cardiac recovery in response to mechanical unloading.

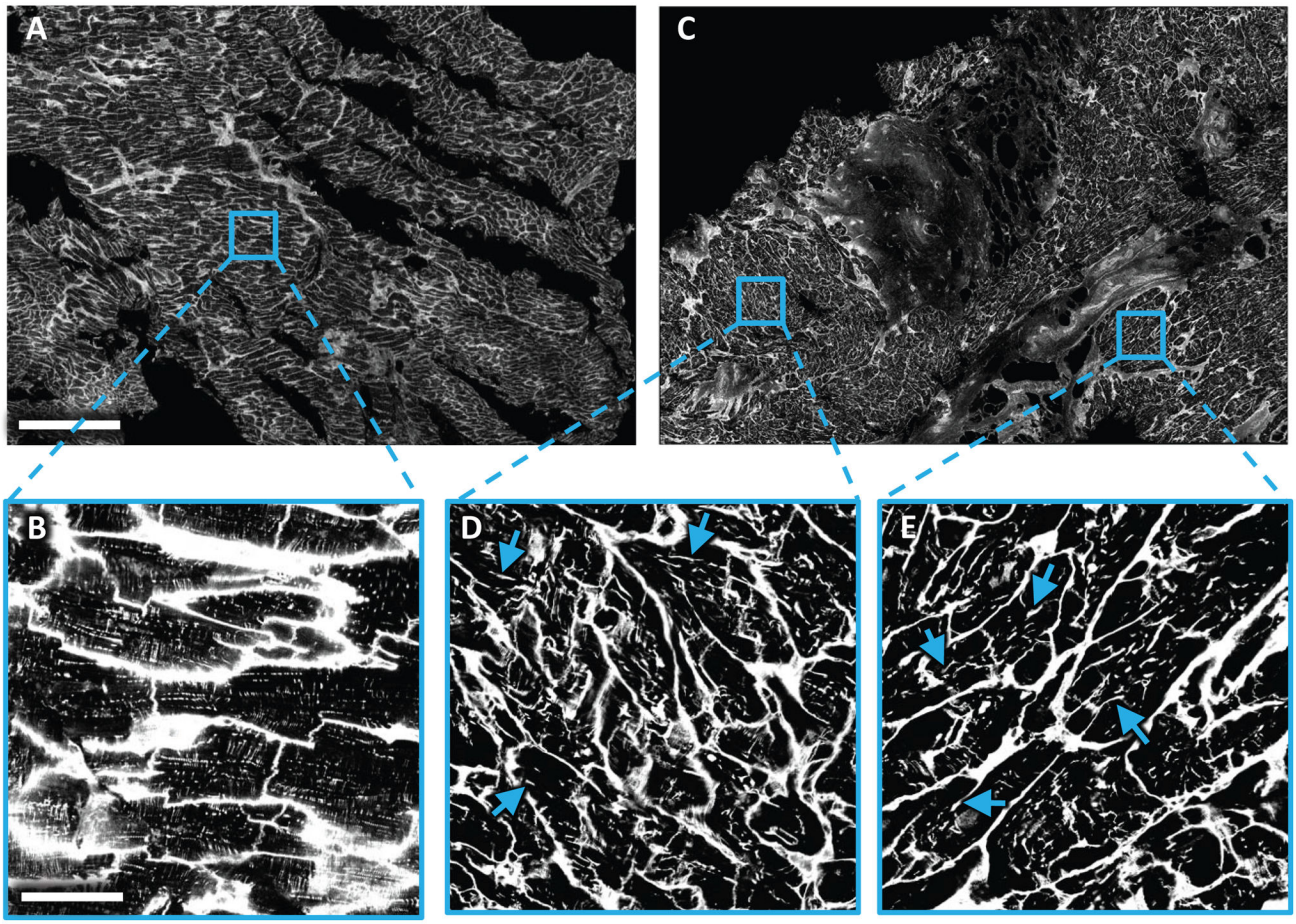

Figure 1. Two-dimensional tile scan of WGA-labeled LV tissue slices obtained from control and HF patient at time of LVAD implantation

Images were acquired with a confocal microscope equipped with a 40× oil immersion lens using a pixel size of 0.2×0.2μm. (A) Tile scan from donor tissue. (B) Magnified view of the boxed region in (A) showing myocytes with dense t-system. (C) Tile scan from HF tissue. (D,E) Magnified views of the boxed region in (C) with myocytes with a sparse and irregular t-system. The remodeled t-system exhibited longitudinal components in the majority of cells. Some examples were marked with arrows. Scale bar in A is 500μm and also applies to C. Scale bar in B is 50μm and also applies to D and E.

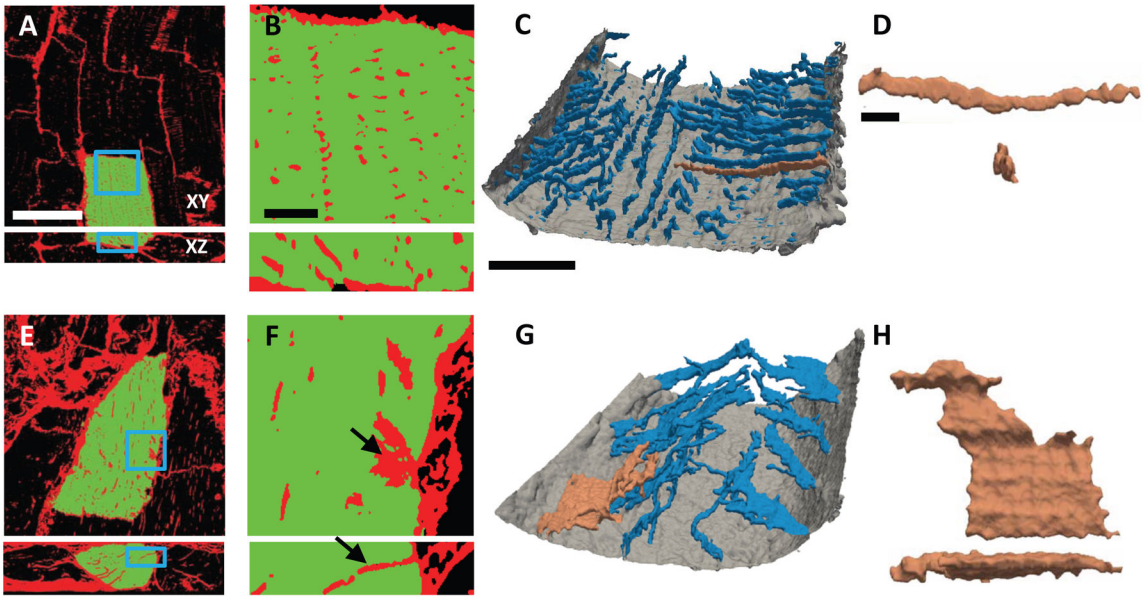

Figure 2. Three-dimensional imaging and reconstruction of t-system from control and HF tissue

(A) Confocal microscopic image from control tissue labeled with WGA (red) for extracellular matrix and sarcolemma. A segmented cardiomyocyte is highlighted in green. (B) Magnified view of the boxed regions in (A) showing myocyte with a dense t-system. (C) 3D reconstruction of outer sarcolemma (gray) and t-system (blue) of a section extracted from the cell highlighted in (A). (D) T-tubule highlighted in (C) shown in longitudinal and transverse view. (E) Image from HF tissue labeled as in (A). A segmented cardiomyocyte is highlighted in green. (F) Magnified view of the boxed region in (E) reveals sparse t-system with sheet-like remodeling. Black arrows point to the same sheet-like component of the t-system. (G) 3D reconstruction of outer sarcolemma (gray) and t-system (blue) of a section from the cell highlighted in (E). (H) Remodeled t-system component highlighted in (G) shown in longitudinal and transverse view.

Scale bar in A: 40μm. Applies to E. Scale bar in B: 5μm. Applies to F. Scale bar in C: 10μm. Applies to G. Scale bar in D: 2μm. Applies to H.

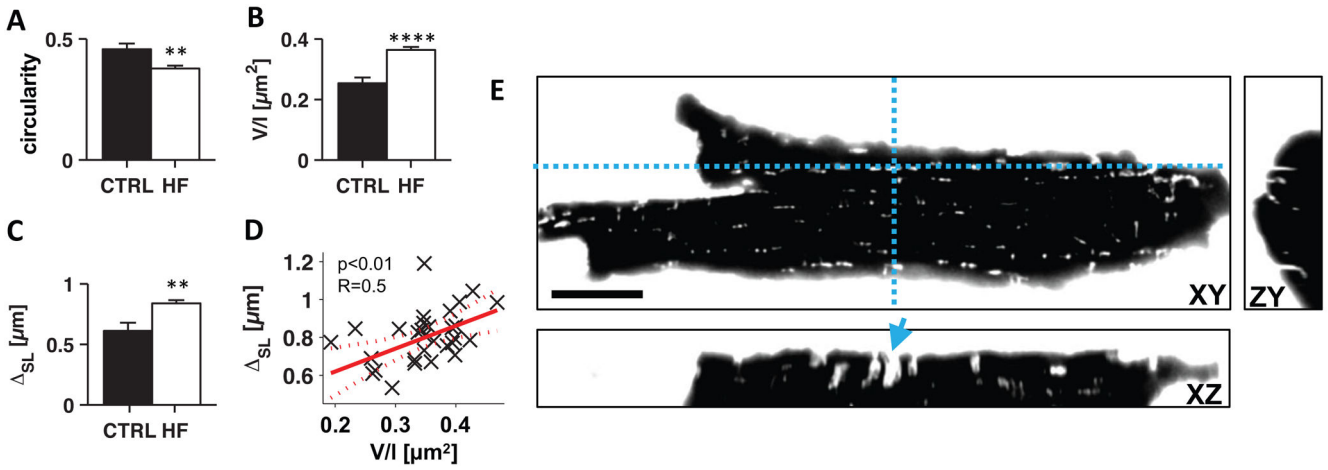

Figure 3. Three-dimensional analyses of t-tubule geometry in control and HF tissue and imaging of isolated cardiomyocytes

Using an extracellular marker confirm remodeling of t-tubules. (A) Cross-sectional circularity of t-tubules, calculated from the two minor eigenvalues $|\lambda_3/\lambda_2|$, was lower in HF (n=26) than in control (n=5). (B) Volume-length ratio (V/l) of t-tubules was increased in HF vs control. (C) Mean intracellular sarcolemma distance (Δ_{SL}) was higher in HF cells than in control cells. (D) Δ_{SL} increased with V/l ($p<0.01$ vs constant model). (E) XY, ZY and XZ cross-sections through three-dimensional image of living isolated cardiomyocyte from HF patient. Dashed blue lines indicate cross-sections. The cell was bathed in 5mg/ml dextran-FITC conjugate (10kDa) as an extracellular marker. Extracellular fluid is shown in white, intracellular space in black. T-sheets were also present in isolated cells (example marked with blue arrow) and exhibited fluorescence, indicating that t-sheet cavities are connected to the extracellular space. Scale bar is 20µm. **p<0.01, ****p<0.0001

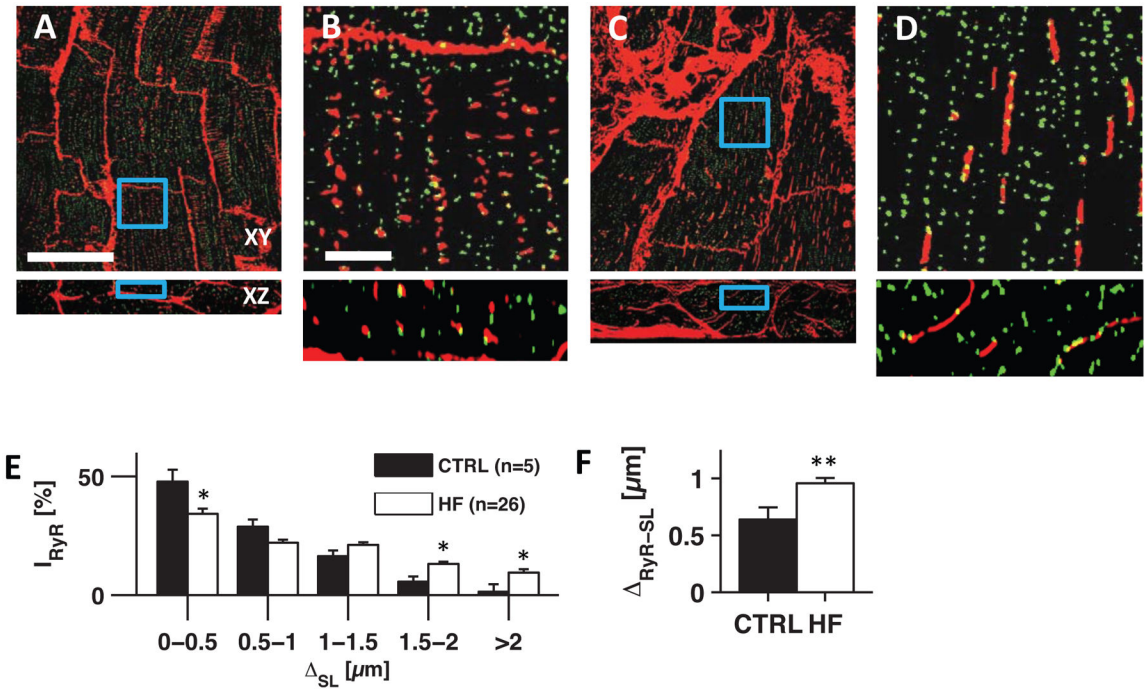

Figure 4. Analyses of RyR-sarcolemma distances in tissue from donors and pre-LVAD patients

Confocal microscopic images of (A) control and (C) HF LV tissue labeled with WGA (red) for extracellular matrix and sarcolemma, and for RyRs (green). (B and D) Magnified view of the boxed regions in (A) and (C), respectively. (E) Fraction of RyR fluorescence intensity (I_{RyR}) found at defined sarcolemma distances (Δ_{SL}) in control (black, n=5) and HF (white, n=26). (F) RyR-sarcolemma distance (Δ_{RyR-SL}) in control and HF.

Scale bar in A: 40μm. Applies to C. Scale bar in B: 5μm. Applies to D. *p<0.05, **p<0.01

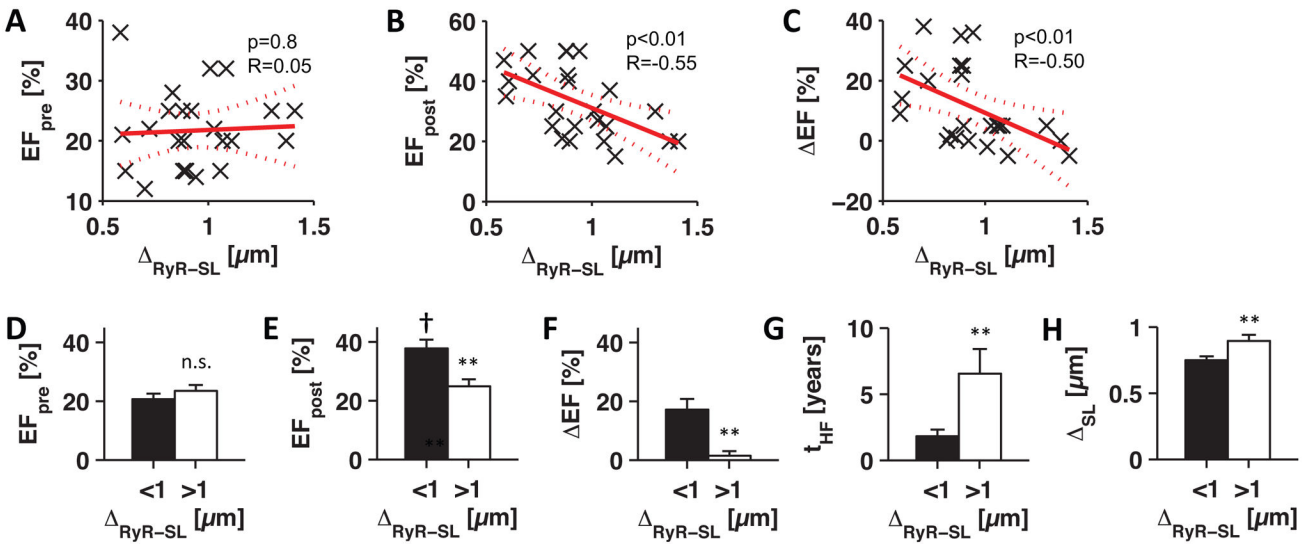

Figure 5. Statistical analyses of clinical and imaging data

Linear regression models of pre-LVAD RyR-sarcolemma distance ($\Delta_{RyR\text{-}SL}$) versus (A) pre-LVAD EF (EF_{pre}), (B) post-LVAD EF (EF_{post}), and (C) EF change during unloading ($\Delta EF = EF_{post} - EF_{pre}$). Significance of F-statistics against constant model is indicated by p and correlation coefficient by R. Dotted lines indicate 95% confidence intervals. (D) pre-LVAD EF, (E) post-LVAD EF, (F) EF change, (G) HF duration (t_{HF}), and (H) sarcolemma distance (Δ_{SL}) in samples from patients grouped by low (<1μm, black, n=16) and high (>1μm, white, n=10) RyR-sarcolemma distance.

**p<0.01 (<1μm vs >1μm), † p<0.001 (EF_{post} vs EF_{pre})

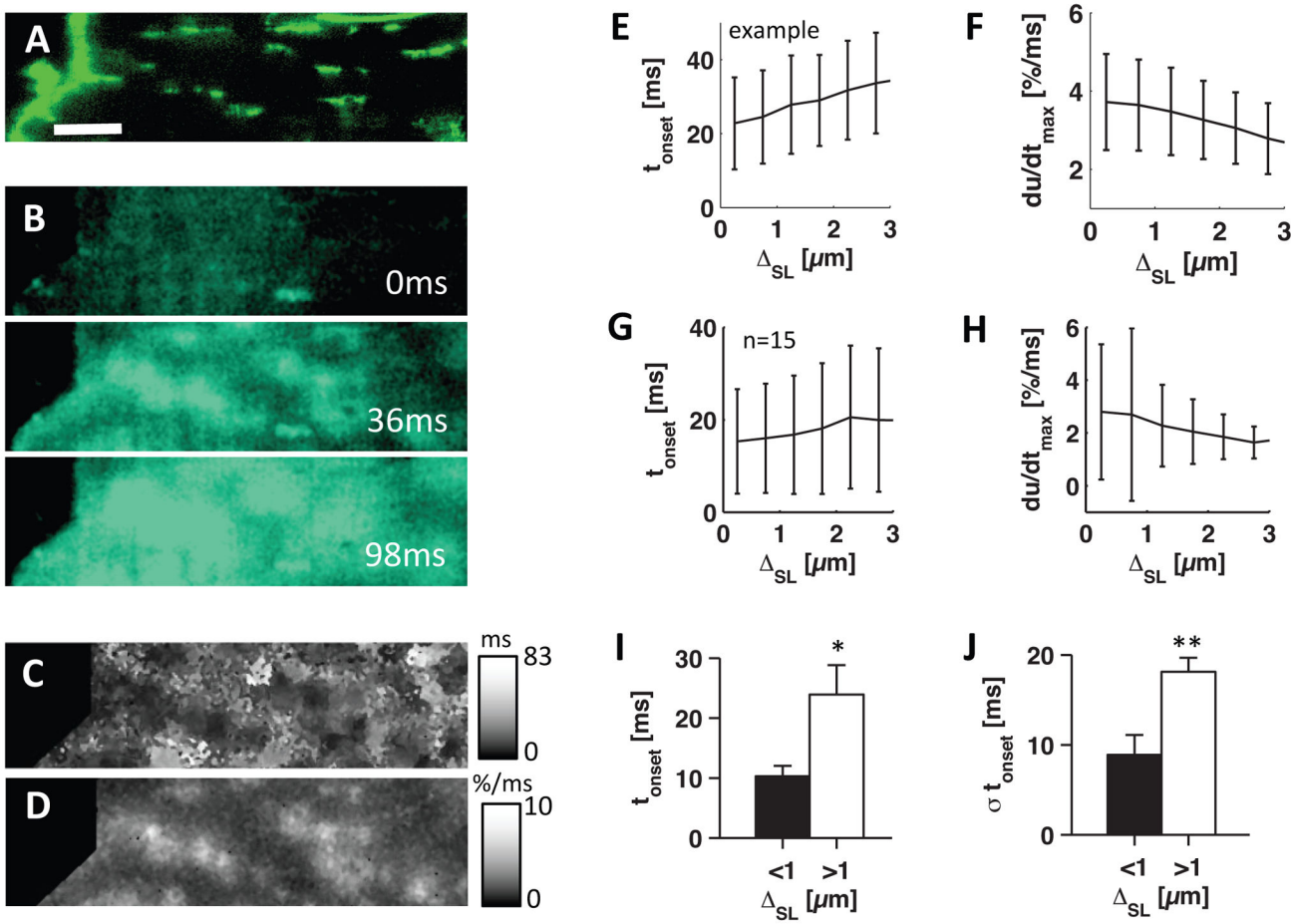

Figure 6. Imaging and analyses of calcium transients in HF cardiomyocytes

(A) Confocal microscopic image of Di-8-ANEPPS labeled isolated myoycte with sheet-like remodeled t-system. (B) Fluo-4 images of cell at time 0, 36 and 98ms after stimulation. (C) Map of onset times of Fluo-4 signal (t_{onset}). (D) Map of maximal upstroke velocities in Fluo-4 signal (du/dt_{max}). (E) Mean±SD of t_{onset} and (F) du/dt_{max} versus sarcolemma distance (Δ_{SL}). Statistical analysis were performed on 15 HF myocytes. (G) Mean±SD of t_{onset} and (H) du/dt_{max} versus Δ_{SL}. (I) t_{onset} and (J) its standard deviation (σt_{onset}) in cells grouped by low (<1μm, black) and high (>1μm, white) Δ_{SL}. Scale bar in A: 10μm. Applies to B–D. *p<0.05, **p<0.01

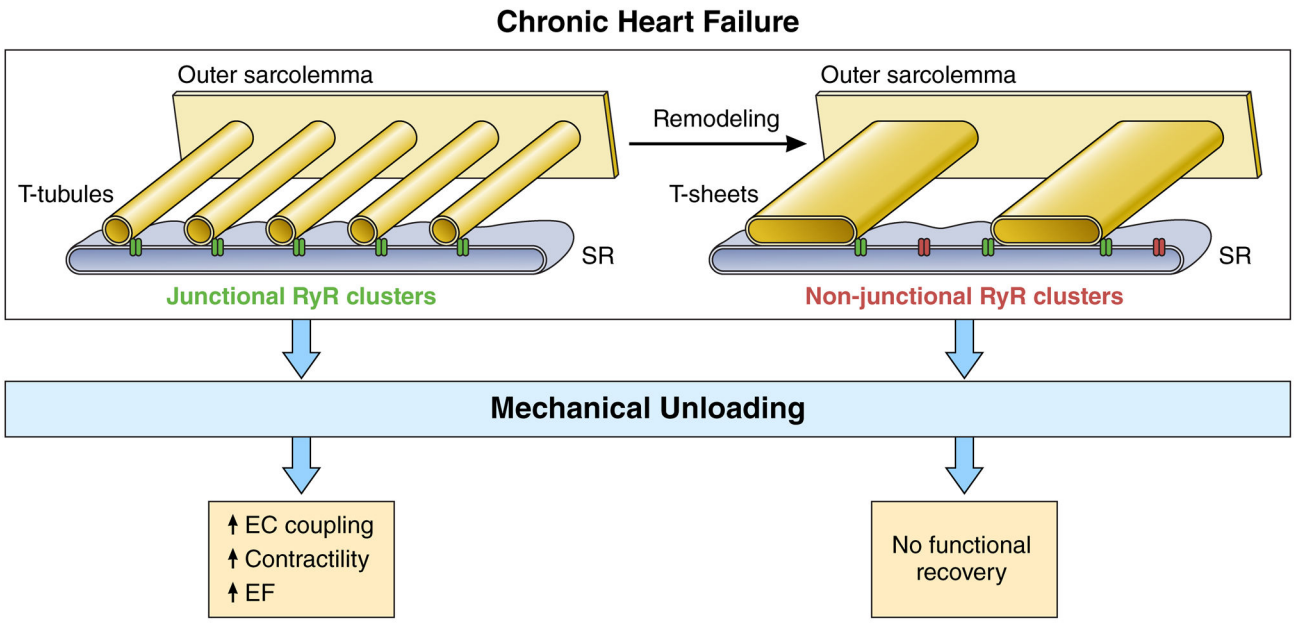

Figure 7. Proposed role of the t-system in functional cardiac recovery in chronic human HF

In some failing hearts, normal t-tubules remodel to t-sheets, t-system components that are significantly widened in the myocyte long axis direction, but still run transversely. Concomitantly, t-system density decreases, which causes a higher fraction of non-junctional ryanodine receptor (RyR) clusters. As a result, triggering of calcium release from the sarcoplasmic reticulum (SR) becomes less efficient. Mechanical unloading by LVAD allows recovery of metabolism[46], beta-adrenergic response[47] and calcium transporters[45], but not of t-system structure[23]. Thus, excitation-contraction (EC) coupling can only recover in failing hearts with a preserved t-system, leading to improved contractility and left-ventricular ejection fraction (EF) following unloading, but not in failing hearts with t-sheets and reduced t-system density.

Table 1

Characteristics of study population before LVAD implantation (n=26).

Age	54±16 years
Male	20 (77%)
NYHA class III	5 (19%)
NYHA class IV	21 (81%)
Duration of HF symptoms	4±4 years
LV EF	21±6%
LV end-diastolic diameter	6.9±1 cm
Cardiac index	2.0±0.4 l/(min·m^2)
Inotrope dependence	15 (58%)
INTERMACS profile	
1	1 (4%)
2	4 (15%)
3	10 (38%)
4	6 (23%)
5	3 (12%)
6	2 (8%)
Chronic HF etiology	
Idiopathic	13 (50%)
Ischemic	10 (38%)
Peripartum	3 (12 %)
Pulmonal Capillary Wedge Pressure	24±10 mmHg
Creatinine	1.3±0.3 mg/dl
B-type natriuretic peptide	1202±949 pg/ml
Hemoglobin	12.4±2.2 g/dl

Data are shown as mean±SD or N (%).